Original Article

Effect of Olanzapine on Pancreas of Adult Male Albino Rats and the Possible Role of Granulocyte Colony Stimulating Factor versus Umbelliferon (A Histological, Immunohistochemical and Biochemical Study)

Samaa M. El Mahrouky[1], Samar Ramzy Mohamed[1], Walaa Samy[2], Sara Mohamed Abdelaal[1]

[1]Department of Medical Histology and Cell Biology, [2]Department of Biochemistry, Faculty of Medicine, Zagazig University, Egypt

ABSTRACT

Introduction: Olanzapine is an atypical antipsychotic prescribed usually for treatment of psychiatric disorders as schizophrenia. It has been widely documented to induce pancreatitis and type 2 diabetes mellitus. Granulocyte colony stimulating factor (G-CSF) is an approved drug for treatment of leucopenia and for mobilization of haemopoietic stem cells from bone marrow towards peripheral circulation. Umbelliferon is a natural plant product that has multiple pharmacological characteristics, including anti-inflammatory, antioxidant, anti-apoptotic and anti-diabetic actions.

Aim of the Work: This research intended to compare the potential therapeutic benefits of umbelliferon and G-CSF on induced pancreatic injury.

Materials and Methods: We utilized forty-eight adult male albino rats that were subdivided into 4 groups; control group, olanzapine group, G-CSF treated group and Umbelliferon treated group. All animals were sacrificed at the end of the experiment and then tissue and serum were gathered for a biochemical analysis. Histological sections from each group were taken and examined under the light and electron microscopes. Results were subjected to morphometrical and statistical studies.

Results: The histological and biochemical results showed different pathological changes of the pancreatic tissue in olanzapine group as distorted acini, thickened septa and congested blood vessels. Also elevated serum amylase and oxidative stress markers as MDA and SOD was shown in the olanzapine group. The GCSF-treated group showed a histological and biochemical improvement, however the structural and biochemical improvement in the umbelliferon group was more than that shown in the G-CSF group.

Conclusions: Finally, we concluded that, umbelliferon administration caused a marked ameliorative effect on olanzapine induced pancreatic injury as a comparable to G-CSF treatment.

Key Words: GCSF, histology, olanzapine, pancreas, umbelliferon.

Revised: 01 July 2024, **Accepted:** 29 July 2024

Corresponding Author: *Samar Ramzy Mohamed*, *Department of Histology and Cell Biology, Faculty of Medicine, Zagazig University, Zagazig, Egypt,* **Tel.:** *+201067013760*, **E-mail:** *drsamarramzy025@gmail.com*

ISSN: 1110-0559, December 2023, Vol. 7, No. 2.

INTRODUCTION

Pancreatitis is an inflammatory disease of the pancreas caused by leakage of activated pancreatic enzymes and leads to disintegration of pancreatic parenchyma[1]. There are two forms of pancreatitis: acute and chronic. Acute pancreatitis is a complicated condition with variable severity and duration. The most common clinical sign is abdominal pain and tenderness[2].

Antipsychotic medications are used to treat bipolar disorder, manic episodes as well as schizophrenia. Schizophrenia is a chronic, severe illness that affects around 21 million people globally. Typically, the most well-known antipsychotics are haloperidol (Haldol) and chlorpromazine (Thorazine). They are still helpful in the treatment of behavioral disorders and severe psychosis. However, a high risk of severe side effects, which is associated with certain drugs. Drug producers created a new class of medications known as atypical antipsychotics in response to these severe adverse effects[3].

On the other hand, one of the most often given atypical antipsychotic medications is olanzapine (OLZ). It is used to treat manic episodes, mixed episodes of bipolar illness, the acute phase and maintenance of schizophrenia and the maintenance of bipolar I disorder[4 - 5].

 DOI: 10.21608/jmh.2024.300588.1131

It has been documented that Olanzapine causes diabetes in both humans and rats through several mechanisms such as the antagonism of H1, α1, α2 and M3 receptors. The antagonism of H1 receptors is leads to weight gain, while M3 receptors' antagonism causes pancreatic damage that result in insulin insufficiency. The pancreatic M3 receptors have a role in regulating the glucose-stimulated cholinergic pathway which releases insulin from the islet of Langerhans beta cells. Olanzapine blocks the pancreatic M3 receptors that reduces the release of insulin and induces hyperglycemia and diabetes[6].

Despite the widespread use of hypoglycemic medications, diabetes and its sequelae remain a significant medical issue. The hypoglycemic drugs have limited efficacy with multiple side effects. Although insulin therapy has a number of disadvantages, including insulin resistance, it is the only effective treatment for diabetes mellitus[7].

While many traditional plants have anti-diabetic properties, only a few have been scientifically tested. The herbal medicine effectiveness is due to their less side effects and affordable price. Umbelliferon (UMB), a derivative of coumarin, mainly extracted from Citrus aurantium. UMB possess pharmacological activities against different diseases, such as degenerative disorders, microbial infections and inflammation[8]. It has been documented that the parent molecule coumarin lowers blood glucose, increases plasma insulin, alters protein composition and cause hypolipidemic impact. Additionally, UMB's are known to activate PPARγ which improves insulin sensitivity and encourages GLUT4 translocation[9].

Numerous researchers have demonstrated that bone marrow mesenchymal stem cells (BMMSCs) can reduce pancreatic damage by developing into pancreatic stem cells. However, it seems that the effects of BMMSC therapy might not be enough because there is a limited supply of BMMSCs that can be transplanted. Also, the inflammatory mediators have an impact on the cells' ability to survive and differentiate after transplantation[10].

Bone marrow hematopoietic stem cells (BMHSCs) can be activated by the hematopoietic cytokine human G-CSF. Thus, it's considered a less costly, more convenient and non-invasive regenerative medicine therapy. Because G-CSF induces a higher rate of stem cell mobilization than spontaneous bone marrow collection, it was chosen for the purpose of HSC mobilization[11 - 12].

The purpose of this research was to investigate and compare the possible therapeutic benefits of neupogen (GCSF) and Umbelliferon on the pancreatic injury induced experimentally.

MATERIALS AND METHODS

Animals:

In this experiment, we used 48 adult male albino rats, from 180 to 200 g weight and 14 to 18 weeks age. The rats were bought from the unit of the animal house of the Zagazig University's Faculty of Medicine. The Zagazig University IACUC Committee was evaluate the protocol and gave it an approval number of (ZU-IACUC/3/F/300 / 2023). A week previous to the experiment, the animals were preserved in clean, stainless-steel crates to allow them to get used to their surroundings. The animals were kept in regular day and night cycles, at room temperature with unrestricted approach to water and food and continued for the full duration of the experiment.

Chemicals:

- *Olanzapine:* (Zyprexa TM) as tablets each of 10 mg purchased from (Eli Lilly Company, Indianapolis, Indiana, USA).
- *Umbelliferon:* It purchased from Sigma-Aldrich (939-35-; Sigma-Aldrich, st. Louis, MO, USA).
- *G-CSF (Neupogen):* 300 µg of recombinant-methionyl human G-CSF (Filgrastim) were contained in each 0.5 ml prefilled syringe. From F. Hoffmann-La Roche Ltd. in Basel, it was acquired. Switzerland's Kirin-Amgen Inc.
- *Experimental design:* Adult male albino rats were used; they were Forty-eight (48) that were subdivided into the following group:

- *Control Group or (group I):*

It contained 24 rats. Three equal subgroups of rats were created:

* *Subgroup IA:* they hadn't received any drugs.

* *Subgroup IB:* the rats were injected by the vehicle of neupogen that was 0.5 ml of 5 % glucose.

* *Subgroup IC:* the rats were fed on 0.5% carboxy methyl cellulose (the vehicle of umbelliferon) by oral gavage.

- *Group II (OLZ-group):*

It included 8 rats that were given 10 mg/kg OLZ orally for 28 days. (Each tablet contained 10 mg of the drug; each tablet was dissolved in 10 ml distilled water, based on that each rat was received about 2 ml of that prepared solution). Animals of this group were sacrificed after 4 weeks[3].

- *Group III (G-CSF group):*

It included 8 rats was given OLZ as in group II, then at the 28th day each rat received SC injections of human recombinant G-CSF at the dose of 100 µg/kg/day, recently dissolved in 0.5 ml of glucose 5 % once daily for 5 consecutive days. After the last injection, we left the animals for further two weeks[13].

* The animals of this group were sacrificed 2 weeks after the last G-CSF injection.

- *Group IV (Umbelliferon, UMB group):*

It included 8 rats that were given OLZ as in group II, then UMB was administrated by oral gavage as following (50 mg/kg of UMB suspended in 0.5 % carboxy methyl cellulose (CMC) once / day for 2 successive weeks[14]. The animals of this group were sacrificed 6 weeks from the start of the experiment.

At the time of scarification, rats were fasted for 12 hours, then they were received an intra-peritoneal injection of 50 mg/ kg body weight of sodium phenobarbital to be anesthetized[15].

Collection of samples:

After animals' euthanizing, the blood samples for biochemical studies were collected in plane tubes. In order to collect the serum, 15 minutes centrifugation of blood samples was performed at 3000 rpm. Storage of the separated serum was performed at - 20° C until time of analysis. Also, the pancreatic tissues were collected from rats of all groups and stored at - 80°C.

Biochemical studies:

- Serum insulin and α-amylase levels were performed using ELISA kits that are commercially available according to manufacturer recommendations (MyBioSource, USA).

- **Estimation of TNF-α and IL-1β (pro-inflammatory cytokines):**

Using ELISA kits (R and D, Minneapolis, MN), the concentrations of pancreatic TNF-α and IL-1β were estimated in the tissue homogenate. It is carried out in compliance with the manufacturer's guidelines.

- **Estimation of the biomarkers of oxidative stress:**

Using commercial assays (bio-diagnostic), the malondialdehyde (MDA) and superoxide dismutase (SOD) concentrations were assessed in the homogenate of the pancreatic tissue as following the manufacturer's guidelines.

Gene Expression Analysis:

The total RNA was extracted from tissue of the pancreas by means of TRIZOL reagent (Invitrogen; Thermo Fisher Scientific, Inc.). Analysis of total RNA was performed to be concentrated and purer, then it is reverse transcribed into cDNA using High-Capacity cDNA Reverse Transcription Kit; (Applied Biosystems™, USA) by following the manufacturer's instructions. Estimation of the expressions of Pdx1, NF-κB-, TLR-4, NLRP-3, NRF2, HO1, NQO1 and RT-PCR was done using Mx3005P (Stratagene, La Jolla, CA, USA) with the TOPrealTM qPCR 2X PreMIX (SYBR Green with low ROX). β-Actin was used as an internal control. All the levels of mRNA were detected by the $2^{-\Delta\Delta ct}$ method. The primers were indicated in Table 1.

Table 1: The list of Primers for Target gene of q RT-PCR:

	Forward (5′-3′)	Reverse (5′-3′)	Accession number	Product size (bp)
Pdx1	GGATGAAATCCACCAAAGCTC	TTCCACTTCATGCGACGGT	>NM_022852.4	244
NF-κB-	AGAGGATGTGGGGTTTCAGG	GCTGAGCATGAAGGTGGATG	>NM_001276711.2	200
TLR-4	CGAGCCAGAATGAGGACTGG	TCCCACTCGAGGTAGGTGTT	>NM_019178.2	352
NLRP-3	GAGCTGGACCTCAGTGACAATGC	ACCAATGCGAGATCCTGACAACAC	>NM_001191642.1	146
NRF2	GCAACTCCAGAAGGAACAGG	GGAATGTCTCTGCCAAAAGC	>NM_001399173.1	203
HO1	ATCGTGCTCGCATGAACACT	CCAACACTGCATTTACATGGC	>NM_012580.2	338
NQO1	ACTCGGAGAACTTTCAGTACC	TTGGAGCAAAGTAGAGTGGT	>NM_017000.3	492
β-actin	CTAAGGCCAACCGTGAAAAGAT	ACCAGAGGCATACAGGGACAAC	>NM_031144.3	104

Histological study:

Light microscopic examination:

After taking of the pancreatic specimens, they were allowed for fixation in 10 % buffered formaldehyde with further processing to finally obtain paraffin sections of 5 μm thickness for Hematoxylin and Eosin (H and E) staining and Mallory trichrome staining[16].

Immunohistochemical staining for insulin protein localization:

As directed by the manufacturer, the avidin biotin complex technique (Cas no. 85878; Sigma-Aldrich, Saint Louis, USA) was used. Paraffin slices thickened to 5 μm were placed on coated slides, dewaxed and then rehydrated. Target proteins were exposed using the antigen retrieval approach, which involved heating citrate buffer to pH 6.0 and 15 microwave cooking it for 15 minutes. The tissues were blocked for half an hour at room temperature using 3 % bovine serum albumin. The anti-insulin primary antibody (mouse monoclonal antibody; No. I 2018; dilution 11000/; Sigma–Aldrich, Steinheim, Germany) was then incubated on them for an additional night at 4°C. Incubation in 10 % H2O2 in phosphate buffered saline (PBS) at pH 7.4 was used to quench endogenous peroxidase. Horseradish peroxidase and biotinylated secondary antibodies were used for detection and 3, 3'-diaminobenzidine (DAB) was used for colorimetric detection after that. The tissues were stained again using Mayer's hematoxylin. The cells expressing insulin exhibited brown cytoplasmic reactions[17].

Electron microscopic examination:

Instantaneous fixation was carried out at pH 7.4 in 2.5 % phosphate-buffered glutaraldehyde. After being post-fixed in the same buffer containing 1 % osmium tetroxide at 4°C, the specimen was dried and embedded in epoxy resin. Using Leica ultracut UCT, ultrathin sections were produced and stained with lead citrate and uranyl acetate[18], then examined and photographed in the Electron Microscope Research Unit, Faculty of Agriculture, Mansoura University, Egypt, using a JEOL JEM-2100 Transmission Electron Microscope (Jeol Ltd., Tokyo, Japan).

Morphometrical analysis:

We made use of a computer system called Leica Qwin 500 image analyzer (Leica Ltd., Cambridge, UK). Using the assistance of a digital camera linked to an optical microscope (Olympus, Tokyo, Japan), the data were examined using Leica QWin 500 software.

From each group of rats, ten non-overlapping fields were selected at random and analyzed to measure:

1. The area % of collagen fibers deposition in sections stained with Masson trichrome stain.

2. The area % of positive insulin immune reaction.

Statistical Analysis:

The collected data from all studied group were presented in the form of means (X) ± standard

deviation (SD). The program used for data analysis was Statistical Package for Social Sciences (SPSS), version 22.0 (IBM Corp., Armonk, NY, USA).

RESULTS

The results of the Biochemical analysis:

Regarding serum insulin level, it was significantly decreased in group II in comparison to control group (I). However, there was a non-significant increase in group III and IV as compared to the group II.

As for serum α Amylase level, it showed a significant increase in group II versus group I. However, it showed a significant decrease in group III and IV in relation to the group II. A non-significant difference was detected between group III and group IV Table 2.

For assessment of inflammation, TNF-α, IL1 beta were assessed in pancreatic tissue and their levels were significantly increased in group II in relation to group I. While, there is a significant decrease was detected in both group III and IV versus group II with more significant decrease in group IV Table 2.

For oxidative stress biomarkers, MDA, SOD levels were assessed in pancreatic tissue. A significant increase in MDA and decrease in SOD levels were noticed in group II as compared to group I. In group III, there was a decrease in MDA and increase in SOD levels non-significantly in comparison to group II. Group IV showed a significant decrease in MDA and increase in SOD levels as compared to group II. However, there was significant decrease in MDA and increase in SOD levels in group IV when compared to group III Table 2.

Table 2: Biochemical analysis of Fasting serum insulin, Seum α Amylase and pancreatic tissue levels of TNF α, IL1 beta, MDA and SOD in studied groups:

	Fasting serum insulin (pg /ml)	Seum α Amylase (U/L)	TNF (ng/g tissue)	Il1 beta (ng/g tissue)	MDA (nmol/g tissue)	SOD (U/mg protein)
Group I (Control)	12.23 ± 3.14	310.11 ± 54.23	125.22 ± 36.21	112.19 ± 29.45	38.21 ± 9.12	400.24 ± 56.10
Group II	6.51 ± 1.21[a]	465.09 ± 66.12[a]	289.14 ± 37.19[a]	354.32 ± 55.32[a]	75.14 ± 10.45[a]	210.23 ± 43.12[a]
Group III	9.25 ± 2.34[a]	396.56 ± 24.45[a, b]	176.16 ± 34.23[a, b]	152.13 ± 28.19[a, b]	42.15 ± 8.56[a]	368.08 ± 48.76[a]
Group IV	7.31 ± 1.18[a]	412.24 ± 36.43[a, b]	234.12 ± 33.12[a, b, c]	231.08 ± 29.45[a, b, c]	59.11 ± 13.21[a, b, c]	287.21 ± 39.57[a, b, c]

[a] significant in comparison to group I.

[b] significant in comparison to group II.

[c] significant in comparison to group III.

Gene expression results:

As for PDX1mRNA levels, their levels were decreased significantly in group II compared to group I, while its expression was increased significantly in both III and IV groups as compared to group II. However, group IV showed more significant increase than group III Table 3.

For NF-κB-, TLR-4, NLRP-3 mRNA levels, there was a significant increase in group II in relation to group I. However, there was a significant decrease in both III and IV groups in relation to group II with more significant decrease in group IV as compared to group III Table 3.

Moreover, for NRF2, HO1, NQO1 mRNA levels, there was a significant decrease in group II when compared to group I. However, there was a significant increase in group III and IV in relation to group II. For NRF2, there was more significant increase in group IV when compared to group III, while there was no significant difference in HO1, NQO1mRNA levels between group III and group IV Table 3).

Table 3: Gene expression analysis of Pdx1, NF-κB-, TLR-4, NLRP-3, NRF2, HO1, NQO1 m RNA levels in the studied groups:

	Pdx1	NF-κB-	TLR-4	NLRP-3	NRF2	HO1	NQO1
Group I (Control)	1.12 ± 0.11	1.05 ± 0.15	1.05 ± 0.19	1.11 ± 0.18	1.09 ± 0.10	1.15 ± 0.16	1.11 ± 0.21
Group II	0.37 ± 0.09[a]	2.58 ± 0.34[a]	4.03 ± 0.39a	3.66 ± 0.44[a]	0.28 ± 0.06[a]	0.43 ± 0.08[a]	0.36 ± 0.08[a]
Group III	0.86 ± 0.13[a, b]	1.43 ± 0.26[a, b]	2.11 ± 0.32[a, b]	1.57 ± 0.21[a, b]	0.79 ± 0.11[a, b]	0.91 ± 0.12[a, b]	0.82 ± 0.12[a, b]
Group IV	0.54 ± 0.10[a, b, c]	1.96 ± 0.31[a, b, c]	3.14 ± 0.47[a, b, c]	2.22 ± 0.35[a, b, c]	0.42 ± 0.09[a, b, c]	0.73 ± 0.14[a, b]	0.69 ± 0.11[a, b]

Histological results:

1. H and E-stained sections:

H and E-stained sections from the Control group showed the normal histological structure of pancreas; closely packed serous acini, separated by thin septa and ducts. Islet of Langerhans appeared as pale oval area Figure 1A. The serous acini have well-defined boundaries and lined by pyramidal cells with rounded basal nuclei. Their cytoplasm showed apical acidophilia and basal basophilia. The islets of Langerhans, cells had pale nuclei and acidophilic cytoplasm Figure 1B.

The OLZ-induced group showed distorted acini with thickened connective tissue septa containing congested blood vessel and dilated duct Figure 2A. Marked thickened connective tissue septa were detected in some sections between the distorted acini Figure 2B. Acini had irregular ill-defined borders and the lining cells had small dark nuclei and vacuolated cytoplasm. The islet of Langerhans was shrunken with dark nuclei Figure 2C. Some sections revealed dilated and congested blood vessels within thick connective tissue septa and fatty infiltration Figure 2D.

Regarding H and E-stained sections of G-CSF treated group, most of acini restored its normal histological appearance but there were relatively thick connective tissue septa appeared with residual mildly congested blood vessel and minimally dilated duct. Islet of Langerhans appeared as pale oval area Figure 3A. Regular serous acini with many cells had apical acidophilic and basal basophilic cytoplasm with basal rounded nuclei. Cells of some acini still had small dark nuclei and vacuolated cytoplasm. A minimally dilated duct and a congested blood vessel were also seen. Islet of Langerhans appeared as pale oval area with most of its cells had pale nuclei Figure 3B.

On the other hand, Umbelliferon-treated group showed apparently normal architecture with closely backed acini separated by thin connective tissue septa containing minimally congested blood vessel. Islet of Langerhans appeared as pale oval area Figure 4A. Most of serous acini with well-defined boundaries; lined by cells with basal basophilic cytoplasm and basal rounded nuclei, apical acidophilic cytoplasm, some cells still having small dark nuclei. Islet of Langerhans' cells had pale nuclei Figure 4B.

2. Mallory trichrome stained sections:

The control group showed scanty collagen fibers deposition within septa, surrounding ducts and blood vessels Figure 1C. OLZ-induced group exhibited extensive deposition of collagen fibers in the septa and around blood vessels Figures 2C and D. Moderate amount of collagen fibers deposition was demonstrated in the septum, around blood vessels and ducts in G-CSF treated group Figures 3C and D. While, Umbelliferon group revealed relatively few collagen fibers within the septa, around ducts and blood vessels Figures 4C and D.

3. Immunohistochemical stained sections:

The control group showed a strong positive immunoreaction in the cytoplasm of central β-cells; negative reactions were found in peripheral non β-cells of the islet of Langerhans Figure 1D. The OLZ- induced group showed an islet of Langerhans with weak cytoplasmic immunoreactions of β-cells Figure 2G. In the G-CSF treated group showed an islet of Langerhans with mild cytoplasmic immunoreactions of β-cells Figure 3E. However, in the Umbelliferon-treated group many B- cells showed moderate cytoplasmic immunoreaction Figure 4E.

4. Transmission Electron Examination:

The TEM examination of the exocrine portion of the pancreas showed acinar cells with basal oval euchromatic nuclei in the control group. The cytoplasm contains numerous electron-dense secretory granules and well-developed rough endoplasmic reticulum Figure 5a. Group II (OLZ-group), showed acinar cells with dark shrunken apoptotic nuclei. Congested blood vessels can be noticed. Large vacuoles within the cytoplasm the acinar cells and sparse less dense granules could be noticed also Figures 5b and c. Group III (G-CSF treated group) showed basal euchromatic nuclei with prominent nucleoli and electron dense secretory

granules and RER. Residual vacuoles were still present Figure 5d. Residual acinar cell with shrunken nucleus were detected. However, other cells appear normal with euchromatic nucleus and dense secretory granules Figure 5e. Group IV (Umbelliferon group), showed marked improvement; the acinar cells had basal euchromatic nuclei, electron-dense granules and well-developed RER Figure 5f.

Examination of β-cells of the islets of Langerhans; the control group showed the β-cells with rounded euchromatic nuclei with prominent nucleoli. Numerous secretory granules with electron dens core and peripheral halos were present in the cytoplasm. Well-developed Golgi apparatus and rough endoplasmic reticulum are noticed. Elongated mitochondria are present all over the cytoplasm Figure 6a. Group II (OLZ group) showed β-cells with heterochromatic nucleus. Many secretory granules appeared with expanded wide peripheral halos. Some cytoplasmic vacuolations and scattered small mitochondria were observed Figure 6b. Also, shrunken apoptotic nuclei, minimal number of secretory granules and cytoplasmic vacuoles were present Figure 6c. Group III (GCSF- treated group) showed oval heterochromatic nuclei. Secretory granules with electron dense core but, some of them lost their limiting membrane. Residual vacuolation was still present Figure 6d. Group IV (Umbelliferon group), showed marked improvement; the β-cells had rounded euchromatic nuclei and numerous secretory granules with electron-dense core. Golgi apparatus and mitochondria are also present Figure 6e.

Morphometrical and statistical analysis:

- The mean value of the area % of collagen fibers showed a high statistically significant increase in groups II (OLZ-group) as compared to other groups. While, the area % of collagen fibers in G-CSF group show a statistically significant increase in comparison to control group. Non-significant difference was detected between the control and Umbelliferon groups Table 4.

- Regarding the mean area % of insulin immunoreaction, there was a statistically significant decrease in OLZ- group in relation to the other groups. A high significant difference was found between the control and G-CSF groups. However, non-significant difference was detected between the control and UMB groups Table 4.

Table 4: The mean area % of collagen fibers and insulin immunoreaction in the different studied groups:

	Control	OLZ- group	GCSF Group	Umbelliferone group	F value	*P* value
Area % of collagen fibers	9 ± 3.49	36.5 ± 5.59	27.4 ± 5.9	13.55 ± 4.15	63.06349	> 0.00001**
Area % of insulin	67 ± 17.05	21.4 ± 7.15	40.6 ± 8.68	54.2 ± 9.23	30.2997	> 0.00001**

** Highly significant *P* value < 0.0001.

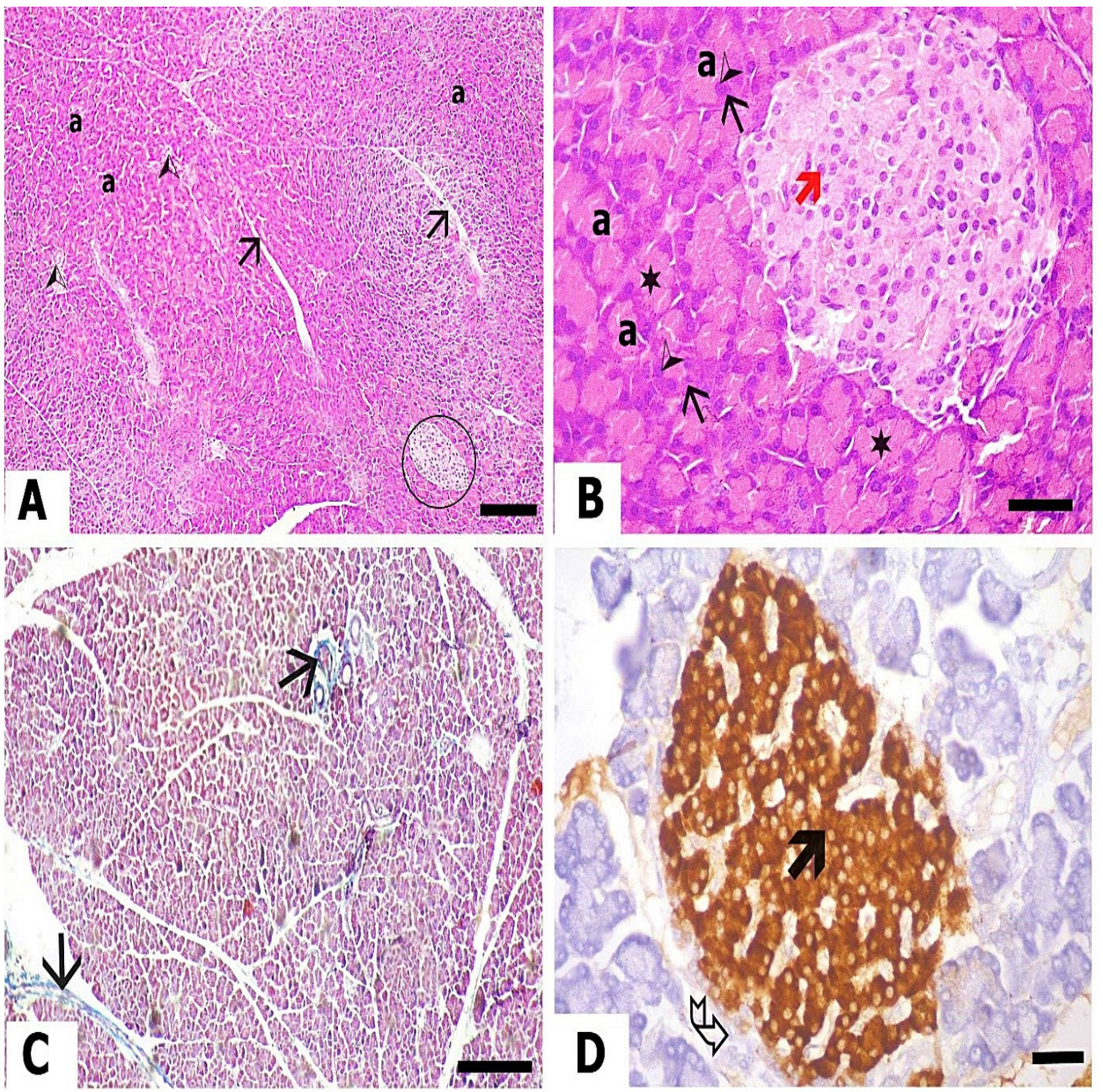

Figure 1: Hematoxylin and Eosin-stained pancreatic sections showing: control group A) General architecture of the pancreas with closely packed serous acini (a); separated by thin septa (arrows); ducts (arrow heads) and an islet of Langerhans (black circle) appears as pale oval area (H and E, x 100, Scale bar; 50 µm). B) Serous acini with well-defined boundaries (a); their lining cells appear pyramidal with basal rounded nuclei (arrow head), apical acidophilic (star) and basal basophilic (arrow) cytoplasm. Cells of islets of Langerhans show pale nuclei (red arrow) and acidophilic cytoplasm (H and E, x 400; scale bar 20 µm). C) Mallory trichrome stained sections of the control group show scanty collagen fibers in the septum, around blood vessels and ducts (arrows) (Mallory's trichrome x 100, Scale bar; 50 µm). D) Strong positive cytoplasmic immunoreactions of the central β-cells (arrow) in the islet of Langerhans; negative reactions of its peripheral non β-cells (curved arrow) (Anti-insulin immune-staining, x 400, scale bar; 20 µm).

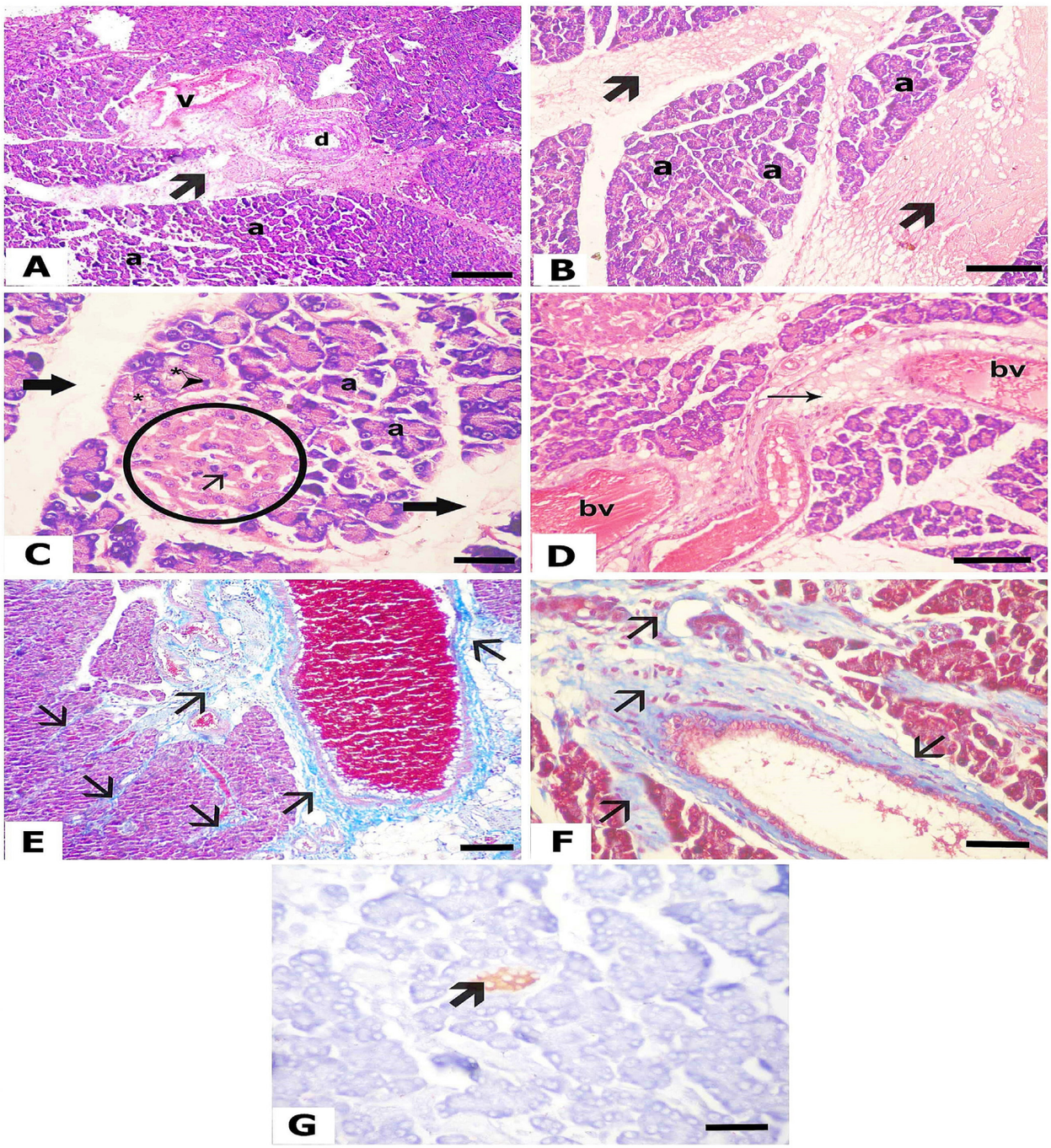

Figure 2: Hematoxylin and Eosin-stained pancreatic sections of OLZ induced group showing A) distorted acini (a) separated by thickened connective tissue septa (arrow) containing congested blood vessel (v) and dilated duct (d) (H and E, x 100, Scale bar; 50 µm). B) Marked thickened connective tissue septa are detected in some sections (arrow) between the distorted acini (a) (H and E, x 400; scale bar 20 µm). C) Acini (a) with irregular ill-defined borders; lined by cells with small dark nuclei (arrow head) and vacuolated cytoplasm (star) separated by thickened septa (thick arrow). Shrunken an islet of Langerhans (black circle) showing dark nuclei (thin arrow) (H and E, x 400; scale bar 20 µm). D) Some sections reveal massive dilated congested blood vessels (bv) with fatty infiltration (arrow) within thick connective tissue fibers deposition (H and E, x 400; scale bar 20 µm). E and F) Extensive collagen fibers showing in the septa and around blood vessels (arrows) (Mallory's trichrome: E x100, Scale bar; 50 µm, F x 400, scale bar; 20 µm). G) Weak cytoplasmic immunoreactions (arrow) of β-cells of an islet of Langerhans (Anti-insulin immune-staining, x 400, scale bar; 20 µm).

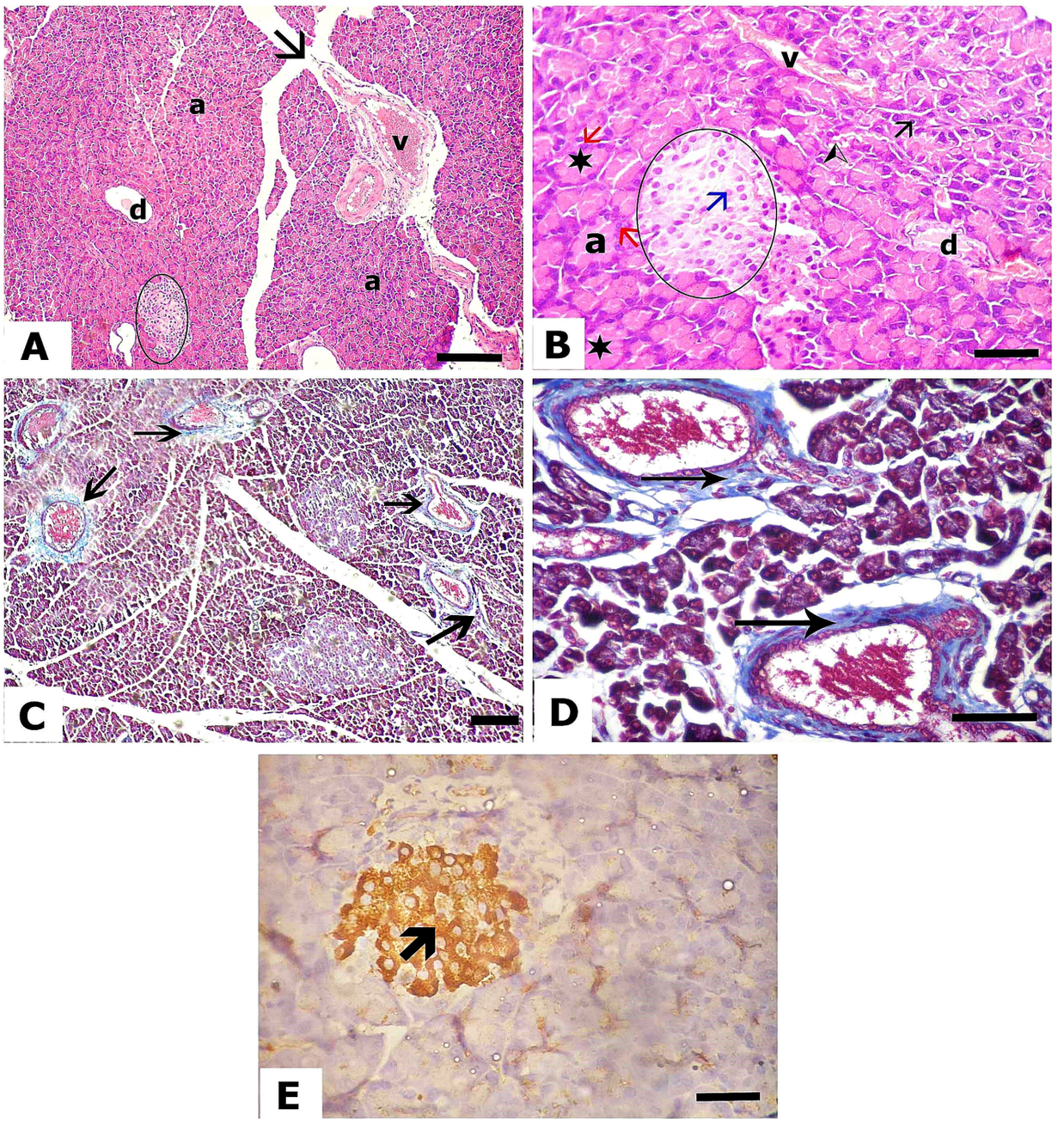

Figure 3: Hematoxylin and Eosin-stained pancreatic sections of G-CSF treated group showing A) restoration of the normal histological appearance of most of acini (a), relatively thick connective tissue septa (arrow) appear with residual mildly congested blood vessel (v) and minimally dilated duct (d). Islet of Langerhans (black circle) appears as pale oval area (H and E, x 100, Scale bar; 50 µm). B). Regular serous acini (a) with many cells have apical acidophilic (star) and basal basophilic cytoplasm with basal rounded nuclei (red arrow). Cells of some acini still have small dark nuclei (black arrow) and vacuolated cytoplasm (arrow head). Minimally dilated duct (d) and a congested blood vessel(v) are also seen. Islet of Langerhans (black circle) appears as pale oval area and most of its cells have pale nuclei (blue arrow). (H and E, x 400; scale bar 20 µm). C and D) Moderate amount of collagen deposition is detected in the septum, around blood vessels and ducts (arrows) (Mallory's trichrome: C x 100, Scale bar; 50 µm, D x 400, scale bar; 20 µm). E) An islet of Langerhans with mild cytoplasmic immunoreactions (arrow) of β-cells (Anti-insulin immune-staining, x 400, scale bar; 20 µm).

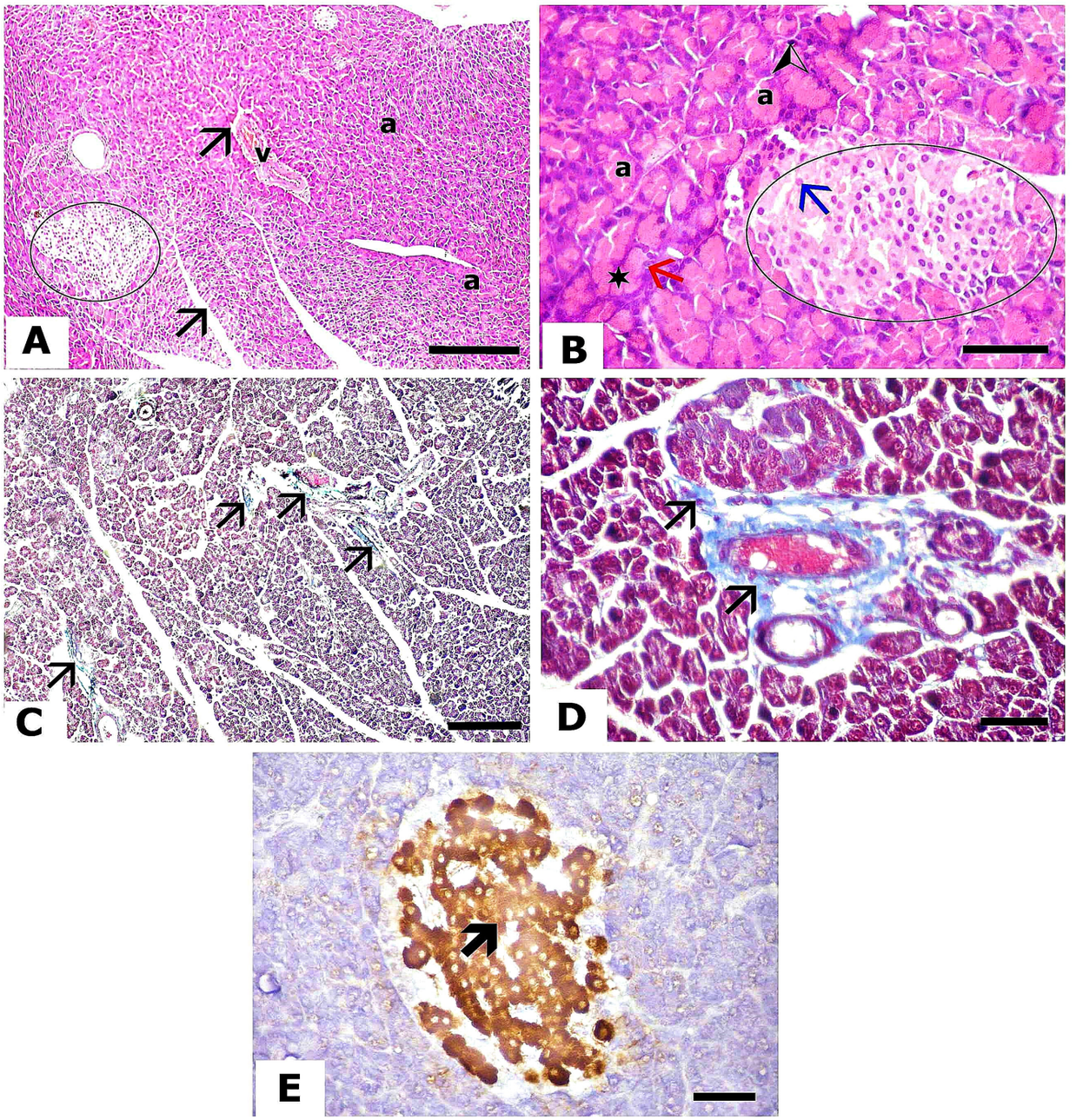

Figure 4: H Hematoxylin and Eosin-stained pancreatic sections of Umbelliferon treated group showing A) apparently normal architecture with closely backed acini (a) separated by thin connective tissue septa (arrow) containing minimally congested blood vessel(v). Islet of Langerhans (black circle) appears as pale oval area (H and E, x 100, Scale bar; 50 µm). B) Most of serous acini (a) with well-defined boundaries; lined by cells with basal basophilic cytoplasm and basal rounded nuclei (red arrow), apical acidophilic cytoplasm (star), some cells still having small dark nuclei (arrow head) (H and E, 400×). An islet of Langerhans shows cells with pale nuclei (blue arrow) (H&E, x 400; scale bar 20 µm). (C and D) Relatively few collagen fibers in the septa and around blood vessels and ducts (arrow) (Mallory's trichrome: C x 100, Scale bar; 50 µm, D x 400, scale bar; 20 µm). E) Moderate cytoplasmic immunoreactions (arrow) in many of the B- cells of islet of Langerhans. (Anti-insulin immune-staining, x 400, scale bar; 20 µm).

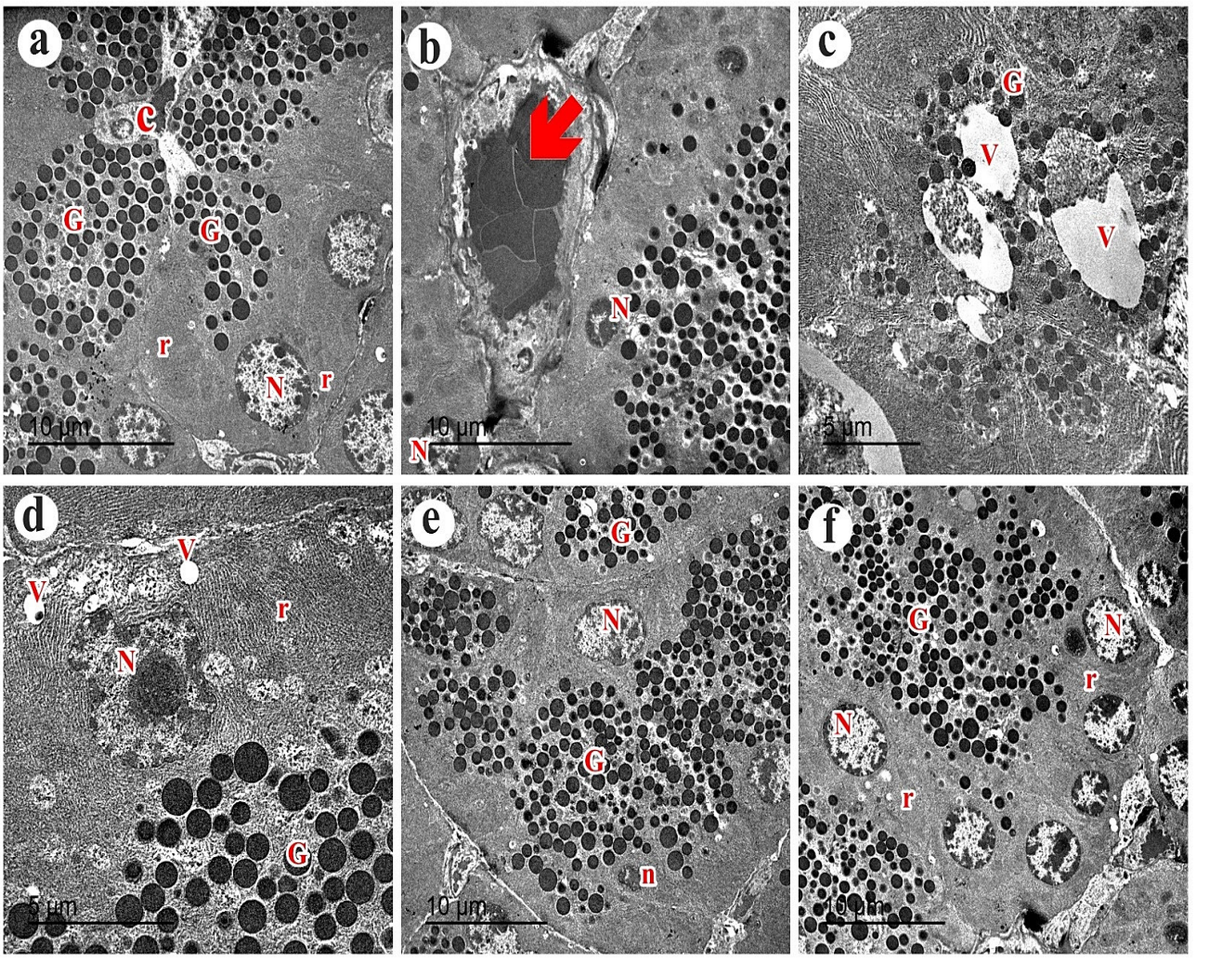

Figure 5: Em picture of exocrine portion of the pancreas of different studied groups showing: (a) Control group showing the acinar cells with basal oval euchromatic nuclei (N). The cytoplasm has numerous electron-dense secretory granules (G) and well-developed RER (r) (TEM, Scale bar 10 µm). (b and c) Group II (OLZ-group); (b) showing acinar cells with shrunken apoptotic nuclei (N). Congested blood vessels can be noticed (arrow) (TEM, Scale bar 10 µm). (c) showing large vacuoles within the cytoplasm the acinar cells (V) and sparse less dense granules (G) (TEM, Scale bar 5 µm). (d and e) Group III (GCSF- treated group); (d) showing basal euchromatic nuclei with prominent nucleoli (N) and electron dense secretory granules (G) and RER (r). Residual vacuoles (v) are still present (TEM, Scale bar 5 µm). (e) showing acinar cell with shrunken nucleus (n). However, other cells appear normal with euchromatic nucleus (N) and dense secretory granules (G) (TEM, Scale bar 10 µm). (f) Group IV (Umbelliferon group), showing marked improvement; the acinar cells have basal euchromatic nuclei (N), electron-dense granules (G) and well-developed RER (r) (TEM, Scale bar 10 µm).

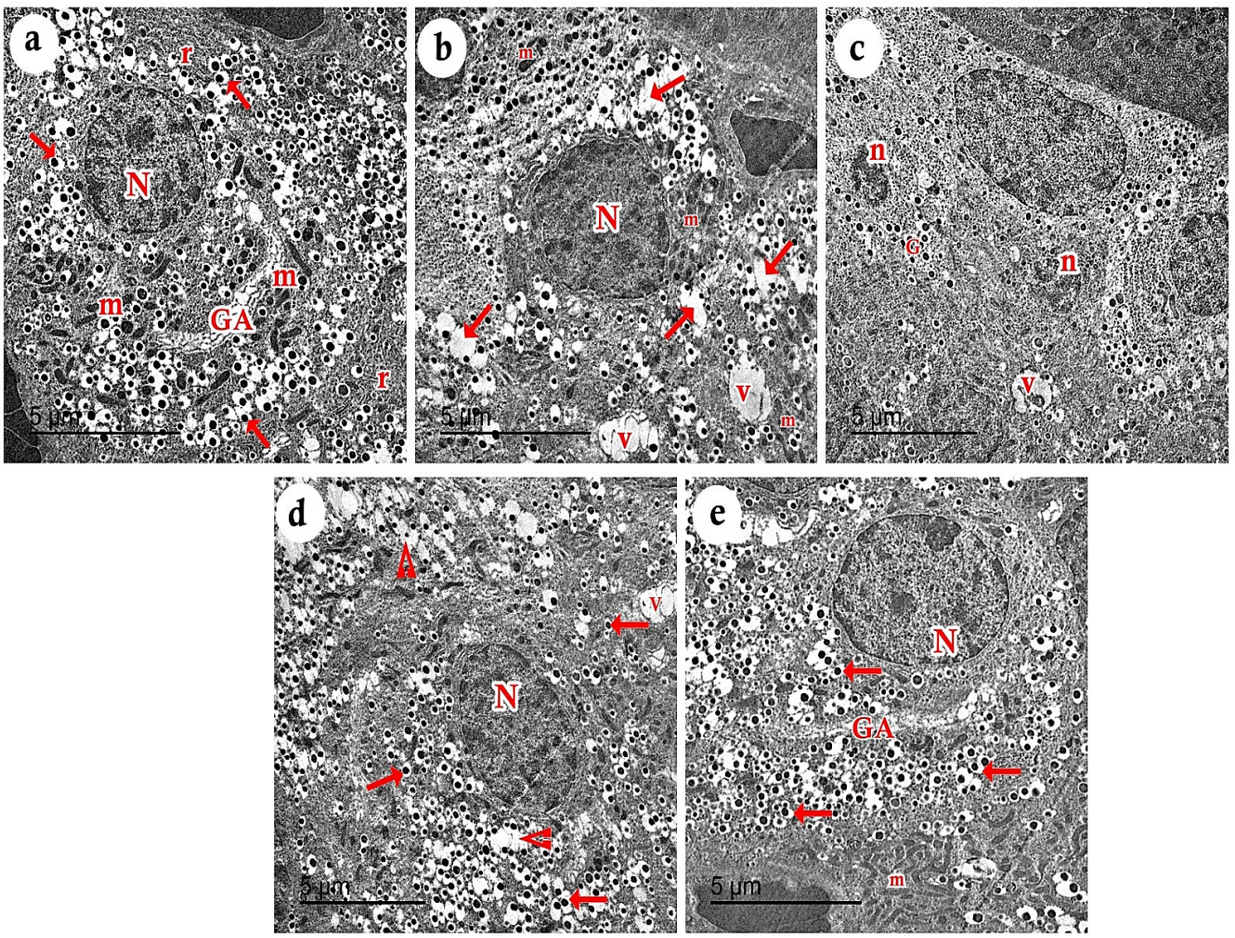

Figure 6: Em picture of β cells in the islets of Langerhans of the pancreas of different studied groups showing: (a) Control group showing the β-cells with rounded euchromatic nuclei with prominent nucleoli (N). The cytoplasm contains numerous secretory granules with electron dens core and peripheral halos (arrows). Well-developed Golgi apparatus (GA) and cisternae of rough endoplasmic reticulum (r) are noticed. Elongated mitochondria are present all over the cytoplasm (m) (TEM, Scale bar 5 µm). (b and c) Group II (Olanzapine group); (b) showing β-cells with heterochromatic nucleus (N). Many secretory granules with expanded wide peripheral halos (arrow). Some cytoplasmic vacuolations (v) and scattered small mitochondria (m) are observed (TEM, Scale bar 5 µm). (c) showing shrunken apoptotic nuclei (n), minimal number of secretory granules (G) and cytoplasmic vacuoles (v) (TEM, Scale bar 5 µm). (d) Group III (GCSF- treated group) showing oval heterochromatic nuclei (N). Secretory granules with electron dense core (arrow) but some of the lost their limiting membrane (arrowheads). Residual vacuolation (v) is still present (TEM, Scale bar 5 µm). (e) Group IV (Umbelliferon group), showing marked improvement; the β-cells have rounded euchromatic nuclei (N) and numerous secretory granules with electron-dense core (arrow). Golgi apparatus (GA) and mitochondria (m) are also present (TEM, Scale bar 5 µm).

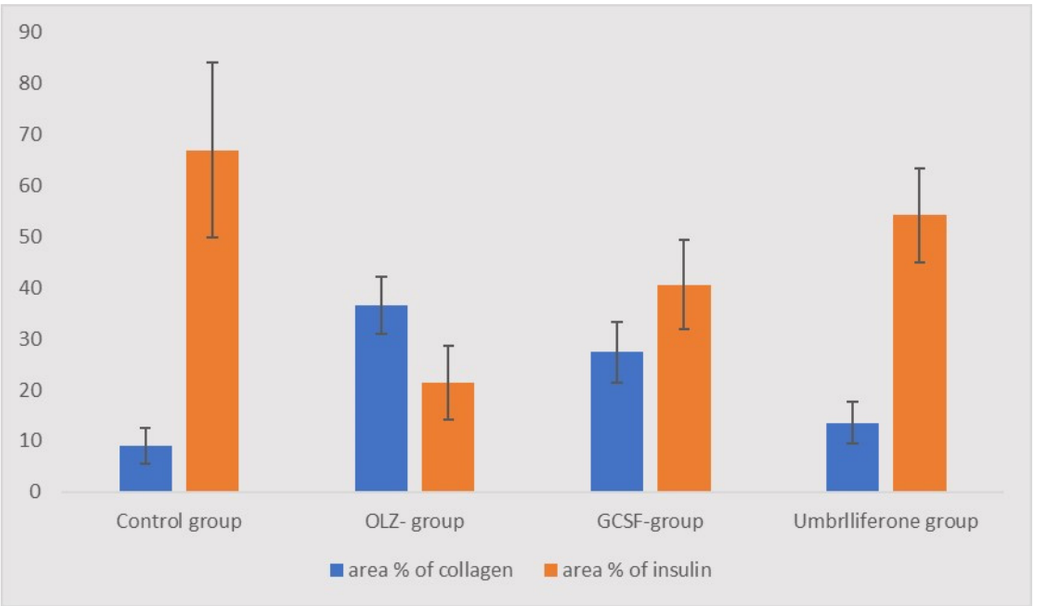

Figure 7: Difference between area % of collagen and area % of insulin among different studied groups.

DISCUSSION

Pancreatitis is an uncommon side effect of antipsychotic use, which can be fatal particularly in patients who have risk factors such as elevated visceral fat, gallstones, hypertriglyceridemia. The risks of pancreatitis are increased with the use of the antipsychotic medications[19].

Umbelliferon (UMB) is a derivative of coumarin that is widely present in different plants including carrot, coriander and lemon. Numerous bioactivities, including antibacterial, antigenotoxic, anti-inflammatory, antioxidant and anticancer properties, are exhibited by UMB[20].

G-CSF performs a variety of actions, as stimulation of proliferation of hematopoietic stem cells and their differentiation and survival. It also induces the mobilization of bone marrow cells into circulation[13].

The goal of our research was to detect the histopathological alterations occur in the pancreas secondary to use of antipsychotic medication olanzapine. Also, to compare the possible ameliorative effect of umbelliferon versus Granulocyte Colony Stimulating Factor.

Group II exhibited a statistically significant reduction in NRF2 mRNA levels as compared to group I. In contrast to group II, there was a noteworthy rise in groups III and IV. Group IV experienced a greater increase in NRF2 than Group III reported. The transcription factor NRF2 is essential for the cell's response to oxidative stress and reactive oxygen species. NRF2 activation has been demonstrated in studies to enhance cellular fitness under stress[21].

Cytosolic KEAP1 constitutively directs NRF2 by the ubiquitin proteasome system for ubiquitylation and degradation. It acts as an adaptor for the E3 ubiquitin ligase Cullin-3 (CUL3) under baseline conditions. Reactive cysteine residues in the KEAP1 structure stop NRF2 from degrading when exposed to oxidative stress. After stabilizing, NRF2 binds to antioxidant-response elements (ARE) into the nucleus to mediate the expression of several genes that code for antioxidant enzymes, including HO-1 and NQO1[22].

Previous research has demonstrated that NRF2 expression dramatically dropped in the pancreatic tissues of mice suffering from acute pancreatitis and has validated the preventive benefits of adjusting NRF2 expression[23].

Group II exhibited a statistically significant increase in NF-κB- and NLRP-3 mRNA levels in comparison to group I. But as compared to group II, there was a significant decline in groups III and IV, with group IV experiencing a greater decrease than group III.

The management of acute pancreatitis depends on suppression of inflammatory processes. In the pancreas, NF-κB is a crucial regulator of genes associated to inflammation[24]. According to Huang *et al.*, (2013)[25], pancreatitis severity in mice is exacerbated by stimulation of cellular NF-κB. Furthermore, a close bond was evidenced between Nrf2 and NF-κB stimulation. According to Jin *et al.*, (2008)[26] and Thimmulappa *et al.*, (2016) [27], Nrf2-deficient mice exhibit high activity for NF-κB and Nrf2 disruption leads to elevated NF-κB activity and increased secretion of proinflammatory cytokine.

The NLRP3 inflammasome has been identified as a key participant in the pathophysiology of AP recently[28]. The current understanding of antioxidants in regulating AP has been deepened by the antioxidant hydrogen's suppression of oxidative stress, which in turn inhibited the NLRP3 inflammasome activation and the IL1ß[29].

Regarding the mRNA levels of PDX1, group II's levels were significantly lower than group I's, however its levels in group III and IV were significantly elevated more than group II's. Group IV, however, displayed a more notable increase than Group III.

Numerous investigations have indicated that PDX-1 is crucial for both insulin secretion and the survival of pancreatic β-cells[30 - 31]. According to findings from another study, MIN6 cells that have PDX-1 inhibited would have a lower survival rate and a higher apoptotic rate[32]. These findings support the role of PDX-1 in controlling insulin release and cell survival.

Examining H and E-stained sections of the OLZ-group revealed disorganized acini separated by thickened connective tissue septa with duct dilation and congestion of blood vessel which were in agreement with Shehata *et al.*, (2022)[33].

Many theories have been proposed to explain the vasodilatation and edema that happened with Olanzapine. Olanzapine blocks α1 and 5HT2 receptors that cause vasodilatation with decreasing vascular resistance and leads to development of edema. Also, increasing cyclic adenosine monophosphate with olanzapine exaggerates vasodilatation. It also alters the renal regulation of fluid and electrolytes through dopaminergic blockage[34].

Sections of the OLZ treated group stained with H and E showed acini with irregular ill-defined boundaries. Vacuolated cytoplasm and small, dark nuclei characterize the cells that line the acini which was in agreement with Elbakary *et al.*, (2017)[35].

The exact mechanism of induction of pancreatitis with olanzapine is unknown. Hyperlipidemia, a documented side effect of olanzapine use, has the potential to trigger severe pancreatitis[36].

Islets of Langerhans are shrunken with dark nuclei. Oxidative stress releases multiple pro-inflammatory cytokines with marked activation of nuclear factor kappa-B and other signaling pathways. Interleukin-1b is the most important cytokine mediator of the destruction of the islets of Langerhans[37].

Additionally, it results in the down-regulation of the glucose transporter 2 (GLUT2) which compromises pancreatic islet's capacity to recognize elevated blood glucose levels, which results in hyperglycemia[38].

Sections of the OLZ treated group's pancreas stained with Mallory's trichrome showed abundant deposition of collagen fibers within the septa and around blood vessels, similar observations were reported by Soliman *et al.*, (2014)[39]. Statistically, these results were verified.

Oxidative stress activates the pancreatic stellate cells (PSCs) leading to their transformation into myofibroblast-like cells[40]. Angiotensin II, IL-1 and platelet-derived growth factor (PDGF) are among additional PSC activators that are elevated. These elements initiate the production of several extracellular matrix proteins by stellate cells that finally cause fibrosis[41 - 42].

Comparing immunostained sections of the OLZ group to the control group in this study, the number of insulin-positive cells was significantly dropped, which is consistent with the findings of Shehata *et al.*, (2022)[33]. Statistical analysis supported these results.

The exact etiology of glucose dysregulation with olanzapine is uncertain. It was hypothesized that 5- HT1A (serotonin) receptors antagonistic effect may decrease the responsiveness of pancreatic beta-cells, that leads to reduction of insulin secretion with resulting hyperglycemia[43].

The TEM sections of OLZ treated group showed minimal number of secretory granules in beta cells. Olanzapine is thought to directly impair the function of pancreatic beta cells, which are the only source of insulin[44 - 45].

Protein misfolding and unfolding are caused by disruptions in the rough endoplasmic reticulum's (RER) function. This condition is known as RER stress; trans-membrane receptors recognize the unfolded protein and trigger the unfolded protein response (UPR) in response. This unfolded protein's breakdown is made worse by the UPR, which promotes the synthesis of ER-resident chaperones[46].

Olanzapine causes a shift in the primary location of proinsulin from insulin granules to the endoplasmic reticulum, which limits insulin production by decreasing proinsulin maturation. Proinsulin misfolding brought on by olanzapine is one of the initial events that cause ER stress in pancreatic beta cells[47].

The OLZ-group's acinar cells' ultrastructural analysis in this study revealed aberrant mitochondria. This finding was made while researching the integrated bioenergetic properties of isolated rat liver mitochondria[48]. This finding aligns with the findings of Shehata *et al.*, (2022)[33]. Mitochondrial changes were explained by deceleration of electron transfer activity at the respiratory complex.

The changes in the endoplasmic reticulum that were detected in this work can be explained as certain atypical antipsychotic drugs disturb Ca++ homeostasis in hepatocytes so induce endoplasmic reticulum stress. This effect was considered one of their metabolic side effects[49].

Ultrastructurally, beta cells of OLZ-treated group revealed reduced numbers of secretory granules and smaller apoptotic nuclei. Due to reduction of free radical scavenging enzymatic system, β-cells are more vulnerable to the harmful effects of NO and ROS molecules. These molecules can damage protein and DNA structures and lead to accelerated apoptosis, as well as diminished secretory ability and insufficient secretory granules in intracellular compartments. Oxidative stress in cells affects both secretory capability and cell viability and both traits result in β-cell failure[50 - 51].

The H and E-stained sections of the G-CSF group demonstrated that most of the serous acini had returned to their normal histological appearance. This is consistent with the findings of Qu *et al.*, (2017)[10], who revealed that in a rat model of acute pancreatitis, the expanded BMMSCs from in vitro could move to the damaged pancreas and multiply there. The histological, biochemical and functional characteristics of the pancreas after the experimental injury are improved by co-administration of G-CSF, while BMMSC transplantation alone demonstrates an efficient role in tissue repair.

Moreover, G-CSF has been shown by Omar *et al.*, (2018)[11] to helps to improve parotid degeneration induced by methotrexate either directly or through stem cells mobilization and telocyte preservation as an additional G-CSF preservation effect. Moreover, this is corroborated by G-CSF's properties as immunomodulation, anti-inflammatory, anti-apoptotic effects and the inhibiting effect of lipid peroxidation[52 - 53].

G-CSF group pancreatic sections stained with Mallory's trichrome revealed moderate collagen fibers deposition in the septa and surrounding ducts and blood vessels. A statistical analysis confirmed these findings.

Umbelliferon is known to exhibit different pharmacological activities against various health-related conditions[8]. The original compound -coumarin- has been approved to have hypoglycemic and hypolipidemic effects with elevation plasma insulin, protein profile. UMB demonstrates a range of pharmacological characteristics in vivo, such as anti-inflammatory and antioxidant effects[54 - 56].

It was demonstrated that by Zambon and Vincent (2008)[57] that UMB has a significant protective effect against induced acute lung injury by blocking TLR-4/Myeloid differentiation primary response 88/NF-κB pathway activation. According to Liu *et al.*, (2017)[58], numerous inflammatory and autoimmune reactions are significantly influenced by the overexpression of NF-κB-p65 signaling.

One of these reactions is NLRP-3; as a vital tissue damage sensor, it plays a role in triggering sterile inflammation. The NLRP-3 inflammasome self-cleaves after activation, activating a range of inflammatory precursors such as TNF-α and IL-1β[59 - 60].

According to Luo *et al.*, (2018)[61], UMB has been implicated in reducing myocardial damage by inhibiting the NLRP-3 inflammasome. Furthermore, a prior study elucidated that the expression of pro-inflammatory cytokines is regulated by TLR-4/NF-kB-p65/NLRP-3 signaling pathway activation[62].

Sim *et al.*, (2015)[55] reported evidence of an anti-inflammatory efficacy of UMB through reduction of the inflammatory cytokines that prevent liver damage induced by alcohol According to Hassanein *et al.*, (2021)[14], TNF-α and IL-1β induced kidney damage was dramatically reduced

with the concomitant administration of gentamycin and UMB. Hassanein *et al.*, (2021)[14] founded that UMB can diminish the TLR-4/NF-κB-p65/NLRP-3 pathway that reduces the inflammatory cytokines production especially TNF-α and IL-1β that cause kidney injury.

Sections of the Umbelliferon-treated group stained with H and E revealed a normal architecture, with closely backed acini divided by thin septa of connective tissue. Between serous acini, the islet of Langerhans was visible as a pale, oval area.

Germoush *et al.*, (2018)[63]; Hassanein *et al.,* (2018)[56] and Mahmoud *et al.*, (2019)[64] have studied the anti-inflammatory and antioxidant properties of UMB against different toxic compounds. UMB increased the expression of PPAR-γ in the liver and strengthened the antioxidant defense mechanisms. A study by Naowaboot *et al.*, (2015)[65] found that diabetic rats given UMB had higher levels of PPAR-γ in their adipose tissue.

The steroid receptor superfamily transcription factor PPAR-γ (peroxisome proliferator-activated receptor gamma) is strongly expressed in the fatty tissue. Modulating glucose as well as lipid metabolism, as well as adipocyte development, are only a few of the numerous biological processes in which PPAR-γ is involved[66]. PPAR-γ activation decreased inflammation and oxidative stress, improved insulin sensitivity, decreased hyperglycemia and dyslipidemia and decreased fat storage[67].

UMB had anti-hyperglycemic effects in rats with type 1 diabetes, as demonstrated by reduced HbA1c levels, improved β cell regeneration and higher insulin release[54, 68]. Through oxidant generation inhibition and Nrf2-mediated antioxidant response up-regulation, UMB reduced oxidative stress and provided protective benefits[69].

In the current study, section of the Umbelliferon group stained with Mallory's trichrome exhibited a little collagen fiber deposited within the septa and around ducts and blood vessels, which was consistent with Shehata *et al.*, (2022)[33]. A statistical analysis was done to confirm these findings. Antioxidant therapy has the potential to reduce collagen deposition in pancreatic disorders.

Mahmoud *et al.*, (2019)[64] also reported that UMB down-regulated the expression of collagen and α-SMA, which reduced fibroblast proliferation and prevented the formation and deposition of fibrous extracellular matrix (ECM). Collagen I, III and ECM proteins are synthesized and released by fibroblasts.

The OLZ treated group, showed a significant elevation in the number of insulin-positive cells as compared to the Umbelliferon treated group in this study which is line with (Kumar *et al.*, 2020 and Shehata *et al.*, 2022)[9, 33]. A statistical verification of these outcomes was conducted.

In rats with type 2 diabetes, eight weeks of UMB therapy decreased blood glucose levels and enhanced insulin production. Adiponectin and the hepatic glucose transporter GLUT-4 were also expressed more frequently. Additionally, it is known that UMBs increase insulin receptor sensitivity and stimulate GLUT-4 translocation by activating PPAR[65].

CONCLUSION AND RECOMMENDATION

Umbelliferon administration caused a marked improvement in olanzapine induced pancreatic injury. Meanwhile, G-CSF could ameliorate the harmful effect of olanzapine on pancreas, but to a lesser extent than umbelliferon. It should also be considered to conduct more researches to determine the ideal method of administration and to adjust the appropriate safe effective dose of Umbelliferon or as an adjuvant drug to the traditional therapies.

CONFLICT OF INTEREST

There is no potential conflict of interest among the authors.

REFERENCES

1. Mederos MA, Reber HA and Girgis MD (2021): Acute pancreatitis: a review. Jama, 325(4), 382-.390 doi:10.1001/jama.2020.20317.

2. Ashraf H, Colombo JP, Marcucci V, Rhoton J and Olowoyo O (2021): A clinical overview of acute and chronic pancreatitis: the medical and surgical management. Cureus, 13(11): e19764. doi: 10.7759/cureus.19764.

3. Ardıç CM, Ilgın S, Baysal M, Karaduman AB, Kılıç V, Aydoğan-Kılıç G and Atlı-Eklioğlu Ö (2021): Olanzapine induced reproductive toxicity in male rats. Scientific Reports, 11(1), 111-. doi: https://doi.org/10.1038/s415984-84235-021-.

4. Zhao J, Jiang K, Li Q, Zhang Y, Cheng Y, Lin Z and Xuan J (2019): Cost-effectiveness of olanzapine in the first-line treatment of schizophrenia in China.

Journal of medical economics, 22(5), 439446-. https://doi.org/10.108013696998.2019.1580714/.

5. Meftah AM, Deckler E, Citrome L and Kantrowitz JT (2020): New discoveries for an old drug: a review of recent olanzapine research. Postgraduate medicine, 132; (1), 8090-. https://doi.org/10.10800/0325481.2019.1701823.

6. Shah R, Subhan F, Sultan SM, Ali G, Ullah I and Ullah S (2018): Comparative evaluation of pancreatic histopathology of rats treated with olanzapine, risperidone and streptozocin. Brazilian Journal of Pharmaceutical Sciences, 54 (03), e17669. https://www.scielo.br/j/bjps/a/MzQG83WkFv9gLxRj3WsnPcS/.

7. El-shaer NH and Nofal AE (2019): The enhancing effect of chamomile on histological and immunohistochemical alterations in diabetic rats. Egyptian Academic Journal of Biological Sciences, D. Histology and Histochemistry, 11(1), 1532-. https://eajbsd.journals.ekb.eg/article_29932.html.

8. Mazimba O (2017): Umbelliferone: Sources, chemistry and bioactivities review. Bulletin of Faculty of Pharmacy, Cairo University, 55(2), 223-232. https://doi.org/10.1016/j.bfopcu.2017.05.001.

9. Kumar K, Satyanarayana M, Narayanaswamy H, Rao S, Prakash, Namarata , Ramesh PT (2020): Evaluation of in vivo Antidiabetic Activity of Umbelliferone in Streptozotocin Induced Diabetic Rats. International Journal of Current Microbiology and Applied Sciences. 9. 352110.20546 .3532-/ijcmas.2020.911.421. https://www.researchgate.net/publication/349448564.

10. Qu, B., Chu, Y., Zhu, F., Wang, B., Liu, T., Yu, B., and Jin, S. (2017): Granulocyte colony-stimulating factor enhances the therapeutic efficacy of bone marrow mesenchymal stem cell transplantation in rats with experimental acute pancreatitis. Oncotarget, 8(13), 21305–21314. https://doi.org/10.18632/oncotarget.15515.

11. Omar AI, Yousry MM, Farag EA (2018): Therapeutic mechanisms of granulocyte-colony stimulating factor in methotrexate-induced parotid lesion in adult rats and possible role of telocytes: a histological study. Egypt J Histol. Mar 1; 41(1):93–107. doi:10.21608/EJH.2018.7525.

12. Alazouny ZM, Alghonamy NM, Mohamed SR and Abdel Aal SM (2022). Mesenchymal stem cells microvesicles versus granulocytes colony stimulating factor efficacy in ameliorating septic induced acute renal cortical injury in adult male albino rats (Histological and Immunohistochemical Study). Ultrastructural Pathology, 46(2), 164187-. https://www.tandfonline.com/doi/abs/10.1080019/13123.2022.2039826.

13. Park IH, Shen GY, Song YS, Cho YJ, Kim BS, Lee Y and Kim KS (2021): Granulocyte colony-stimulating factor reduces the endoplasmic reticulum stress in a rat model of diabetic cardiomyopathy. Endocrine Journal, 68(11), 1293.1301- https://doi.org/10.1507/endocrj.EJ210016-.

14. Hassanein EH, Ali FE, Kozman MR and Abd El-Ghafar OA (2021): Umbelliferone attenuates gentamicin-induced renal toxicity by suppression of TLR-4/NF-κB-p65/NLRP-3 and JAK1/STAT-3 signaling pathways. Environmental Science and Pollution Research, 28(9), 1155811571-. DOI: 10.1007/s113565-11416-020-.

15. Wen L, Gao Q, Ma CW, Ge Y, You L, Liu RH, ... and Liu D (2016): Effect of polysaccharides from Tremella fuciformis on UV-induced photoaging. Journal of Functional Foods, 20, 400410-. https://doi.org/10.1016/j.jff.2015.11.014.

16. Suvarna KS, Layton C and Bancroft JD (2018): editors. Bancroft's Theory and Practice of Histological Techniques E-Book.: Elsevier Health Sciences; 8th edition, China; p: 126137-.

17. Hafez S, Zaghloul D and Caceci T (2015): Immunohistochemical identification of the endocrine cells in the pancreatic islets of the camel, horse and cattle. Eur J Anat. 19 (1):27–35.

18. Tizro P, Choi C, Khanlou N (2019): Sample preparation for transmission electron microscopy. Biobanking: methods and protocols, 1897: 417–424. DOI: 10.100733_5-8935-4939-1-978/.

19. Silva MA, Key S, Han E and Malloy MJ (2016): Acute pancreatitis associated with an-tipsychotic medication: evaluation of clinical features, treatment and polypharmacy in a series of cases. J. Clin. Psychopharmacol. 36, 169–172. DOI: 10.1097/JCP.0000000000000459.

20. Ali FE, Hassanein EH, El-Bahrawy AH, Omar ZM, Rashwan EK, Abdel-Wahab BA and Abd-Elhamid TH (2021): Nephroprotective effect of umbelliferone against cisplatin-induced kidney damage is mediated by regulation of NRF2, cytoglobin, SIRT1/FOXO-3 and NF-kB-p65

signaling pathways. Journal of Biochemical and Molecular Toxicology, 35(5), e22738. https://doi.org/10.1002/jbt.22738.

21. Cloer EW, Goldfarb D, Schrank TP, Weissman BE and Major MB (2019): NRF2 activation in cancer: from DNA to protein. Cancer research, 79(5), 889.898-https://doi.org/10.11585472-0008/.CAN-182723-.

22. Kobayashi A, Kang MI, Watai Y, Tong KI, Shibata T, Uchida K and Yamamoto M (2006): Oxidative and electrophilic stresses activate Nrf2 through inhibition of ubiquitination activity of Keap1. Molecular and cellular biology, 26(1), 22127 .229-https://doi.org/10.1128/MCB.26.1.221229.2006-.

23. Liu X, Zhu Q, Zhang M, Yin T, Xu R, Xiao W, ... and Ding Y (2018): Isoliquiritigenin ameliorates acute pancreatitis in mice via inhibition of oxidative stress and modulation of the Nrf2/HO-1 pathway. Oxidative medicine and cellular longevity, 2018:7161592. https://doi.org/10.11557161592/2018/.

24. Bhatia M, Brady M, Shokuhi S, Christmas S, Neoptolemos JP and Slavin P (2000):"Inflammatory mediators in acute pancreatitis," The Journal of Pathology, vol. 190, no. 2, pp. 117–125.

25. Huang H, Liu Y, Daniluk J, Gaiser S, Chu J, Wang H, ... and Ji B (2013): Activation of nuclear factor-κB in acinar cells increases the severity of pancreatitis in mice. Gastroenterology, 144(1), 202.210-.

26. Jin W, Wang H, Yan W, Xu L, Wang X, Zhao X, ... and Ji Y (2008): Disruption of Nrf2 enhances upregulation of nuclear factor-B activity, proinflammatory cytokines and intercellular adhesion molecule-1 in the brain after traumatic brain injury. Mediators of inflammation, Article ID 725174, 7 pages, 2008.

27. Thimmulappa RK, Lee H, Rangasamy T, Reddy SP, Yamamoto M., Kensler TW and Biswal S (2016): Nrf2 is a critical regulator of the innate immune response and survival during experimental sepsis. The Journal of clinical investigation, 116(4), 984.995-.

28. Hoque R, Sohail M, Malik A, Sarwar S, Luo Y, Shah A, ... and Mehal W (2011): TLR9 and the NLRP3 inflammasome link acinar cell death with inflammation in acute pancreatitis. Gastroenterology, 141(1), 358.369-. https://doi.org/10.1053/j.gastro.2011.03.041.

29. Ren JD, Ma J, Hou J, Xiao WJ, Jin WH, Wu J and Fan KH (2014): Hydrogen-rich saline inhibits NLRP3 inflammasome activation and attenuates experimental acute pancreatitis in mice. Mediators of inflammation, 2014, Article ID 930894, 9 pages, 2014. https://doi.org/10.1155930894/2014/.

30. Claiborn KC, Sachdeva MM, Cannon CE, Groff DN, Singer JD, Stoffers DA (2010): Pcif1 modulates Pdx1 protein stability and pancreatic beta-cell function and survival in mice. J Clin Invest. 120:3713–21.

31. Li Y, Cao X, Li L, Brubaker P, Edlund H and Drucker D (2005): Cell Pdx1 expression is essential for the glucoregulatory, proliferative and cytoprotective actions of glucagon-like peptide-1. Diabetes.; 54:482–91.

32. Hung T, Piia H, Zhiqiang H, et al. (2007): Suppression of Pdx1 in MIN6 cells reduces cell survival and growth by altering expression of genes that regulate apoptosis and cell cycle progression. Diabetes. 1 pA411.

33. Shehata AS, Zidan RA, El-Mahroky SM and Abd El-Baset SA (2022): Efficacy of platelet rich plasma on pancreatic injury induced by renal ischemia reperfusion in adult male rats. Ultrastructural Pathology, 46(2), 188.203- https://doi.org/10.1080 01913123.2022.2044945/.

34. Cook EA, Shipman D. and Fowler TG. (2020): Whole-body edema with olanzapine: a case report and literature review. Mental Health Clinician, 10(5), 291.295-.

35. Elbakary RH (2017): Histological Study of the Effects of Olanzapine on the Liver of Adult Male Albino Rat with and without Vitamin C. the Egyptian Journal of Histology, 40; (1); 111-.

36. Üçok A and Gaebel W (2008): Side effects of atypical antipsychotics: A brief overview. World Psychiatry, 7 (1), 58- 62. doi: 10.1002/j.2051-5545.2008.tb00154.x.

37. Rani AJ, Mythili SV (2014): Study on and total antioxidant status in relation to oxidative stress in type 2 diabetes mellitus. Journal of Clinical and Diagnostic Research, 8(3): 108110-. doi: 10.7860/JCDR/20147603.4121/.

38. Burke SJ, Stadler K, Lu D, Gleason E, Han A, Donohoe DR, ... and Collier JJ (2015): IL-1β reciprocally regulates chemokine and insulin secretion in pancreatic β-cells via NF-κB. American Journal of Physiology-Endocrinology

and Metabolism, 309(8): E715-E726. doi: 10.1152/ajpendo.00153.2015.

39. Soliman, MES, Kefafy, MA, Mansour MA, Ali AF and Esa WAII (2014): Histological study on the possible protective effect of pentoxifylline on pancreatic acini of l-arginine-induced acute pancreatitis in adult male albino rats. Menoufia Medical Journal, 27(4): 801808-.

40. Siech M, Zhou Z, Zhou S, Bair B, Alt A, Hamm S, ... and Bachem MG (2009): Stimulation of stellate cells by injured acinar cells: a model of acute pancreatitis induced by alcohol and fat (VLDL). American Journal of Physiology-Gastrointestinal and Liver Physiology, 297(6), G1163-G1171. DOI: 10.1152/ajpgi.90468.2008.

41. Ryu GR, Lee E, Chun HJ, Yoon KH, Ko SH, Ahn YB and Song KH2013)): Oxidative stress plays a role in high glucose-induced activation of pancreatic stellate cells. Biochemical and biophysical research communications, 439(2): 258263-. https://doi.org/10.1016/j.bbrc.2013.08.046.

42. Hamada S, Masamune A and Shimosegawa T (2015): Pancreatic fibrosis. Pancreapedia: The Exocrine Pancreas Knowledge Base. DOI: 10.3998/panc.2015.42.

43. Chiu C, Chen C, Chen B, Yu S and Mong-Liang L (2010): The time-dependent change of insulin secretion in schizophrenic patients treated with olanzapine. Progress in Neuro-Psychopharmacology and Biological Psychiatry, 34, 866870-. doi:10.1016/j.pnpbp.2010.04.003.

44. Nagamine T. (2014): Does olanzapine impair pancreatic beta-cell function directly? Clinical Neuropsychopharmacology and Therapeutics 5:23–25. DOI: https://doi.org/10.5234/cnpt.5.23.

45. Nagamine T. (2018): Olanzapine and diabetic ketoacidosis: what is the underlying mechanism? Innovations in Clinical Neuroscience 15:11. PMID: 29707419.

46. Minamino T, Komuro I and Kitakaze M (2010): Endoplasmic reticulum stress as a therapeutic target in cardiovascular disease. Circ. Res. 107(9):1071–1082. https://doi.org/10.1161/CIRCRESAHA.110.227819.

47. Ninagawa, S., Tada, S., Okumura, M., Inoguchi, K., Kinoshita, M., Kanemura, S., et al., (2020). Antipsychotic olanzapine-induced misfolding of proinsulin in the endoplasmic reticulum accounts for atypical development of diabetes. Elife, 9, e60970. DOI:10.7554/elife.60970.

48. Modica-Napolitano JS, Lagace CJ, Brennan WA and Aprille JR (2003): Differential effects of typical and atypical neuroleptics on mitochondrial function in vitro. Arch Pharm Res.; 26(11):951-959. DOI:10.1007/BF02980205.

49. Lauressergues E, Bert E, Duriez P, Hum D, Majd Z, Staels B and Cussac D (2012): Does endoplasmic reticulum stress participate in APD-induced hepatic metabolic dysregulation? Neuropharmacology; 62(2):784 -796. https://doi.org/10.1016/j.neuropharm.2011.08.048.

50. Newsholme P, Morgan D, Rebelato E, Oliveira-Emilio HC, Procopio J, Curi R and Carpinelli A (2009): Insights into the critical role of NADPH oxidase(s) in the normal and dysregulated pancreatic beta cell. Diabetologia 52(12):2489–2498. https://doi.org/10.1007/s001251536--009-z.

51. Gorasia DG, Dudek NL, Veith PD, Shankar R, Safavi-Hemami H, Williamson NA and Purcell AW (2015): Pancreatic beta cells are highly susceptible to oxidative and ER stresses during the development of diabetes. Journal of proteome research, 14(2): 688699-. https://doi.org/10.1021/pr500643h.

52. Kang W, Liu ZW, Han QY, Zhang L, Lei Y and Lou S (2008): Effects of granulocyte colony-stimulating factor on hepatocyte apoptosis in acute liver failure: experiment with rats. Zhonghua Yi Xue Za Zhi (Chin Med J); 88(14): 980–984. PMID: 18756972.

53. Hou XW, Jiang Y, Wang LF, Xu HY, Lin HM, He XY, ... and Zhang S (2009): Protective role of granulocyte colony-stimulating factor against adriamycin induced cardiac, renal and hepatic toxicities. Toxicology letters, 187(1), 40.44- https://doi.org/10.1016/j.toxlet.2009.01.025.

54. Ramesh B, Pugalendi KV. Antihyperglycemic effect of umbelliferone in streptozotocin-diabetic rats. J Med Food 2006; 9: 562–6. doi: 10.1089/jmf.2006.9.562.

55. Sim MO, Lee HI, Ham JR et al (2015): Anti-inflammatory and antioxidant effects of umbelliferone in chronic alcohol-fed rats. Nutr Res Pract ; 9:364–369. doi: 10.4162/nrp.2015.9.4.364.

56. Hassanein, E. H., Mohamed, W.R., Shalkami, A.G.S., Khalaf, M. M. and Hemeida, R. A. (2018): Renoprotective effects of umbelliferone on methotrexate-induced renal injury through

regulation of Nrf-2/Keap-1, P38MAPK/NF-κB and apoptosis signaling pathways. Food and Chemical Toxicology, 116, 152.160-.

57. Zambon M, Vincent JL (2008): Mortality rates for patients with acute lung injury/ARDS have decreased over time. Chest 133:1120–1127. https://doi.org/10.1378/chest.072134-.

58. Liu T, Zhang L, Joo D, Sun SC (2017): NF-κB signaling in inflammation. Signal Transduct Target Ther 2:17023. https://doi.org/10.1038/sigtrans.2017.23.

59. Mezzasoma L, Antognelli C and Talesa VN (2016): Atrial natriuretic peptide down-regulates LPS/ATP-mediated IL-1β release by inhibiting NFkB, NLRP3 inflammasome and caspase-1 activation in THP-1 cells. Immunol Res 64:303–312. https://doi.org/10.1007/s120260-8751 015--.

60. Afonina IS, Zhong Z, Karin M and Beyaert R (2017): Limiting inflammationthe negative regulation of NF-κB and the NLRP3 inflammasome. Nat Immunol 18:861–869. https://doi.org/10.1038/ni.3772.

61. Luo H, Fan Z, Xiang D, Jiang Z, Zhang W, Gao L, Feng C (2018): The protective effect of umbelliferon ameliorates myocardial injury following ischemia-reperfusion in the rat through suppression NLRP3 inflammasome and upregulating the PPAR-γ Molecular medicine reports 17:34043410- https://doi.org/10.3892/mmr.2017.8208.

62. He X, Wei Z, Wang J, Kou J, Liu W, Fu Y, Yang Z (2016): Alpinetin attenuates inflammatory responses by suppressing TLR4 and NLRP3 signaling pathways in DSS-induced acute colitis. Sci Rep 6:28370. https://doi.org/10.1038/srep28370.

63. Germoush MO, Othman SI, Al-Qaraawi MA et al. (2018): Umbelliferone prevents oxidative stress, inflammation and hematological alterations and modulates glutamate-nitric oxide-cGMP signaling in hyperammonemic rats. Biomed Pharmacother; 102: 392–402.

64. Mahmoud AM, Hozayen WG, Hasan IH et al. (2019): Umbelliferone Ameliorates CCl4-induced liver fibrosis in Rats by upregulating PPARγ and attenuating oxidative stress, inflammation and TGF-β1/Smad3 Signaling. Inflammation; 42: 1103–16. doi: 10.1007/s107538-00973-019-.

65. Naowaboot J, Somparn N, Saentaweesuk S et al. (2015): Umbelliferone improves an impaired Glucose and Lipid Metabolism in High-Fat Diet/Streptozotocin-Induced Type 2 Diabetic Rats. Phytother Res; 29:1388–95. doi: 10.1002/ptr.5392.

66. Han L, Shen WJ, Bittner S et al. (2017): PPARs: regulators of metabolism and as therapeutic targets in cardiovascular disease. Part II: PPAR-β/δ and PPAR-γ. Fut Cardiol; 13: 279–96. doi: 10.2217/fca-20170019-.

67. Zhang Q, Liu T, Ng CY et al. (2014): Diabetes mellitus and atrial remodeling: mechanisms and potential upstream therapies. Cardiovasc Therap ; 32: 233–41. doi: 10.11115922.12089-1755/.

68. Ramu RS, Shirahatti PS, NS et al. (2016): Assessment of in Vivo antidiabetic properties of umbelliferon and lupeol constituents of Banana (Musa sp.var. Nanjangud Rasa Bale) flower in hyperglycaemic rodent model. PLoSOne; 11: e0151135. doi: 10.1371/journal.pone.0151135.

69. YIN J, Wang H and Lu, G (2018): Umbelliferon alleviates hepatic injury in diabetic db/db mice via inhibiting inflammatory response and activating Nrf2-mediated antioxidant. Bioscience reports, 38(4), BSR20180444.

الملخص العربي

تأثير الأولانزابين على بنكرياس الجرذان المهق البالغة والدور المحتمل للعامل المحفز لمستعمرات الخلايا المحببة مقابل الأمبيليفيرون (دراسة نسيجية وهستوكيميائية مناعية وكيميائية حيوية)

سماء محمد المحروقي[1]، سمر رمزى محمد[1]، ولاء سامي[2]، سارة محمد عبد العال[1]

[1]قسم الهستولوجيا الطبية وبيولوجيا الخلية ـ [2]قسم الكيمياء الحيوية ـ كلية الطب البشري ـ جامعة الزقازيق

مقدمة البحث: أولانزابين هو مضاد للذهان غير تقليدي يوصف عادة لعلاج الاضطرابات النفسية مثل الفصام. وقد تم توثيقه على نطاق واسع للحث على التهاب البنكرياس ومرض السكري من النوع الثانى. العامل المحفز لمستعمرات الخلايا المحببة هو دواء معتمد لعلاج نقص الكريات البيضاء ولتعبئة الخلايا الجذعية المكونة للدم من نخاع العظم نحو الدورة الدموية الطرفية. الأمبيليفيرون هو منتج نباتي طبيعي له خصائص دوائية متعددة، التي تشمل مضادات الالتهاب، ومضادات الأكسدة، ومضادات موت الخلايا المبرمج، ومضادات مرض السكري.

الهدف من البحث: يهدف هذا البحث إلى مقارنة الفوائد العلاجية المحتملة للأمبيليفيرون والعامل المحفز لمستعمرة الخلايا المحببة على إصابة البنكرياس المستحثة بدواء الأولانزابين.

المواد والطرق: وقد تم استخدام استخدمنا 48 جرذا ذكرًا بالغًا، تم تقسيمهم مقسمة إلى أربع مجموعات؛ الضابطة، مجموعات الأولانزابين، العامل المحفز لمستعمرات الخلايا المحببة وأمبيليفيرون. تم التضحية بجميع الحيوانات، ثم جمعت الأنسجة والمصل لإجراء التحليل الكيميائي الحيوي. تم فحص مقاطع من كل مجموعة تحت المجهر الضوئي والإلكتروني تليها الدراسات المورفومترية والإحصائية.

النتائج: أظهرت النتائج النسيجية والكيميائية الحيوية تغيرات مرضية في أنسجة البنكرياس لمجموعة الأولانزابين. أظهرت مجموعة الأمبيليفيرون تحسنًا نسجيًا وكيميائيًا حيويًا أكثر من ذلك الذي ظهر في مجموعة العامل المحفز لمستعمرات الخلايا المحببة.

الاستنتاج: تسبب إعطاء الأمبيليفيرون في تحسن ملحوظ فى نسيج البنكرياس مقارنة بالعامل المحفز لمستعمرات الخلايا المحببة فى حالة إصابة البنكرياس الناجمة عن الأولانزابين.